Materials Science-Poland, *Vol. 27*, *No. 1*, *2009*

Structure, magnetic and electrical transport properties of $Mn_{4-x}Ag_xN$ compounds

W.J. FENG[1, 2*], D. LI[1], Q. ZHANG[1], Y.F. DENG[2], S. MA[1], Z.D. ZHANG[1]

[1] Shenyang National Laboratory for Materials Science, Institute of Metal Research, and International Centre for Materials Physics, Chinese Academy of Sciences, Shenyang 110015, China

[2] Shenyang-Chelyabinsk Laboratory of Condensed Matter Physics, College of Physics and Technology, Shenyang Normal University, Shenyang 110034, China

$Mn_{4-x}Ag_xN$ compounds (x = 0.0, 0.3, 0.6, 1.0) were prepared by milling and subsequently annealing the mixture of $Mn_2N_{0.86}$, Mn, and Ag powders. All compounds display good single-phase characteristics. Both Mn_4N and $Mn_{3.7}Ag_{0.3}N$ exhibit ferrimagnetism, and a little Ag replacement of Mn can improve the saturation magnetization. The magnetic transition of $Mn_{3.4}Ag_{0.6}N$ and Mn_3AgN below 15 K is from triangular antiferromagnetism to non-coplanar ferrimagnetism, while the ones at 256 and 275 K ($Mn_{3.4}Ag_{0.6}N$ and Mn_3AgN, respectively) have been ascribed to the gradual transition, as temperature increases, from the triangular antiferromagnetic structure Γ^{5g} to a ferrimagnetic-like one. Two minima appear on the $\rho(T)$ curves for Mn_3AgN, with the observation of a positive magnetoresistance throughout the whole tempeature-dependent change.

Key words: *antiferromagnetism; spin reorientation; magnetoresistance*

1. Introduction

Nitrogen atoms in octohedral interstices of fcc manganese yield the cubic anti-perovskite Mn_4N and, in turn, produce a strong difference between the Mn atoms surrounding the nitrogen and those at the corners of the unit cell. Therefore, the face centred Mn forms an Mn_6N octahedron having a great chemical stability [1]. Conversely, Mn atoms at the corners have greater lability, hence can be substituted by a set of metallic atoms, giving rise to the family of the anti-perovskite Mn_3MN (M = Zn, Cu, and Sn, etc.) compounds [2–4].

Mah [5] prepared Mn_4N, with a minor impurity phase MnO, by heating Mn powders in N_2 for 31 h at 1173–1243 K, and determined the heat of combustion of Mn_4N

*Corresponding author, e-mail: wjfeng@yahoo.com.cn

as –441.4±0.2 kcal/mol. Takei et al. [6, 7] determined its magnetic structure by means of neutron diffraction. At 77 K, the Mn moments with $3.85\mu_B$, at the corner of the cubic unit cell, are anti-parallel to three face-centred moments of $0.90\mu_B$. Recently, the film of Mn_4N [8] was grown by plasma-based ion implantation, and the corresponding structural and magnetic properties were extensively investigated. On the other hand, Fruchart et al. [9] reported the preparation of Mn_3AgN compound. Their investigation revealed that the manganese moment of the Mn_3AgN compound was 3.1 μ_B below 55 K, with a coexistence of two kinds of triangular antiferromagnetic (AFM) structures, i.e. Γ^{4g} and Γ^{5g}, which indicated the presence of ferromagnetic moments. However, this compound exhibits a pure triangular AFM structure Γ^{5g} in the temperature range between 55 and 290 K, with the manganese moment of 2.8 μ_B. After considering the magneto-crystalline anisotropy energy and the Dzyaloshii–Moriya interaction, Gomonaj et al. [10] stated that the magnetic phase transition at low temperatures of Mn_3AgN should be from triangular AFM to non-complanar ferrimagnetic (FIM n.c.) ones. Moreover, Mn_4N and its various metal-doped compounds such as $Mn_{4-x}Ga_xN$ [11] and $Mn_3(Cu_{1-x}Ge_x)N$ [12, 13] display a variety of magnetic structures as well as promising applications.

From the aforementioned research, it can be inferred that $Mn_{4-x}Ag_xN$ with $x = 0 – 1$ solid solution compounds could be produced successfully. Moreover, from the ferrimagnetism of Mn_4N to a pure triangular AFM structure Γ^{5g} of Mn_3AgN, it is a significant and interesting subject to explore magnetic and transport properties of $Mn_{4-x}Ag_xN$ solid solution compounds which might lead to some new findings as well as applications.

2. Experimental details

Mn flakes were milled under an argon atmosphere for 5 h in a high-energy ball mill. The as-milled powders were firstly homogenized at 573 K in a vacuum for 20 min and then cooled down to room temperature. N_2 was introduced into the enclosed tube with the powders, before in-situ nitrogenation was carried out at 823 K for 4 h. X-ray diffraction (XRD) pattern reveals a single-phase compound $Mn_2N_{0.86}$ [14]. Mn, Ag and $Mn_2N_{0.86}$ powders were mixed evenly in an appropriate proportion. The powder mixtures were continuously milled under an argon atmosphere for 1 h before interruption at a predetermined interval of 0.5 h, so as to prevent $Mn_2N_{0.86}$ from decomposition. The total milling time was 5 h. The as-milled powders were annealed at 823 K for 30 min in a vacuum better than 2×10^{-3} Pa.

XRD analysis was performed using CuK_α radiation with a Rigaku D/max-γA rotating target diffractometer. Magnetic properties were investigated with a superconducting quantum-interference device (SQUID, Quantum Design). For the magnetic measurements, the sample was cooled from 295 K to 5 K in the absence of a magnetic field and subsequently subjected to a dc magnetic field at 5 K. The sample was then heated while the magnetization was measured in the constant field. The powders were

uniformly solidified with glue. The powders were pressed into a pellet that was ground to a rectangular parallelepiped with the dimensions of $1\times0.6\times8$ mm^3 to fit the test holder used for electrical measurement. Temperature dependences of electrical resistivity were measured by a standard four-probe method.

3. Results and discussion

3.1. Structural properties

Figure 1 shows the XRD patterns of $Mn_{4-x}Ag_xN$ compounds. The diffraction peaks of all the compounds are broadened indicating the presence of nanocrystallites. All samples are isostructural with Mn_4N ($Pm\bar{3}m$). As mentioned above, Mn atoms at the corner of Mn_4N have greater liability than those at the face centre, and may be

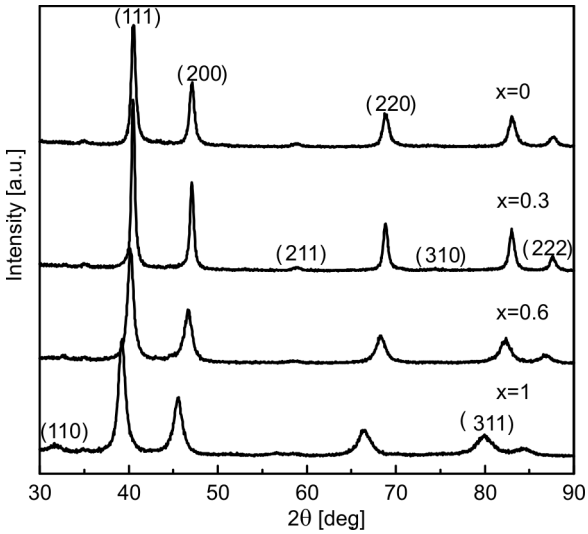

Fig. 1. X-ray diffraction patterns of $Mn_{4-x}Ag_xN$ with x = 0.0, 0.3, 0.6, and 1.0

preferentially substituted, which is confirmed by a successful preparation of $Mn_{4-x}Ag_xN$ solid solution compounds. Besides, with the increase of Ag content, the corresponding XRD peaks of the compounds shift towards lower angles which indicates lattice expansion. Due to a smaller atomic radius of Mn (0.1365 nm) than that of Ag (0.1445 nm), the change of lattice parameters of the $Mn_{4-x}Ag_xN$ compound is entirely reasonable.

3.2. Magnetic properties

Temperature dependences of magnetizations of Mn_4N and $Mn_{3.7}Ag_{0.3}N$ compounds under dc magnetic fields of 10 mT and 5 T (only for Mn_4N) are plotted in

Fig. 2. Obviously, both curves under the field of 10 mT display similar behaviour. A broad peak occurs in the range from 5 to 300 K. However, the temperature dependence of magnetization under the field of 5 T represents no abnormal behaviour in the same temperature range. The isofield magnetizations of Mn_4N, or rather $Mn_{4-x}In_xN$ with $x = 0$ with a large magnetic field [15] resemble that of ours under the field of 5 T. Therefore, the round cusp should be ascribed to a spin reorientation.

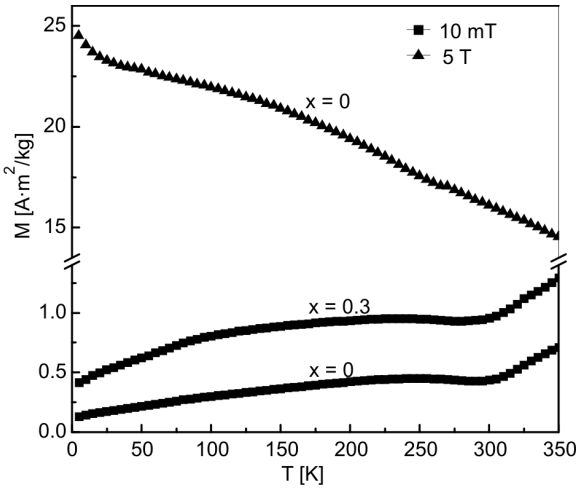

Fig. 2. Temperature dependences of magnetization of $Mn_{4-x}Ag_xN$ ($x = 0$, 0.3) measured in a dc magnetic field of 10 mT and 5 T

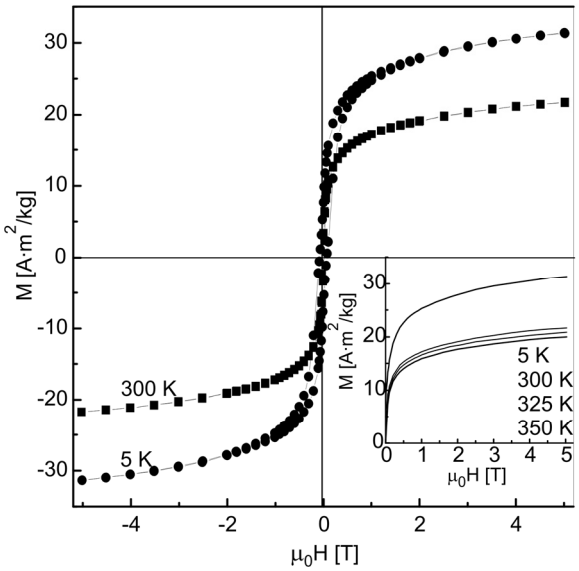

Fig. 3. Hysteresis loops of $Mn_{3.7}Ag_{0.3}N$ at 5 and 300 K. The inset shows the isothermal magnetization curves at different temperatures

The hysteresis loops of $Mn_{3.7}Ag_{0.3}N$ compounds at 5 and 300 K are shown in Fig. 3. Its inset gives isothermal magnetizations at various temperatures. Ferrimagnetic behaviour can be observed for this compound in the temperature range 5–350 K. It is well known that Mn_4N exhibits ferrimagnetism [6, 7]. Moreover, weakly Ag substituted Mn_4N compound can still display ferrimagnetism. Furthermore, as shown in Figs. 2 and 3, the saturation magnetizations at 5 K of Mn_4N and $Mn_{3.7}Ag_{0.3}N$ are 24.8 and 31.7 $A \cdot m^2/kg$.

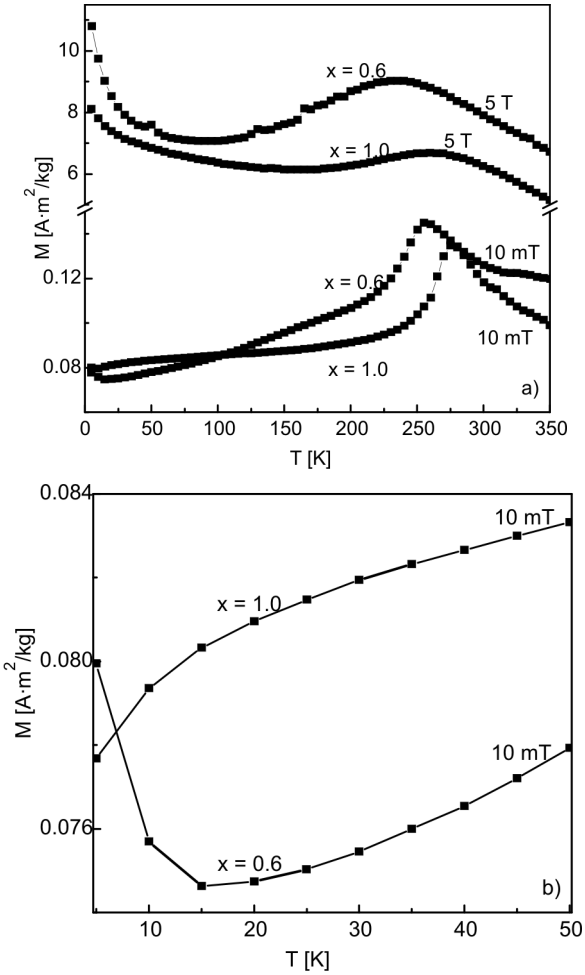

Fig. 4. Temperature dependences of magnetization of $Mn_{4-x}Ag_xN$ (x = 0.6, 1.0) measured in a dc magnetic field of 10 mT and 5 Tat a) 300 K, b) 5 K

Spin reorientation can be often observed in the Mn_3MN family (M = Ag, Ga, Ni, etc.) [10, 16, 17]. That is, the presence of weak ferromagnetism or triangular AFM is based on the symmetry of Γ_{4g} or Γ_{5g}, or their combined magnetic structures, i.e. rotation of triangular magnetic moment in the (111) crystal plane. During the rotation

process, the axis would change continuously in a wide temperature interval without changes in the magnitude of moments or in the lattice structure, and then spin reorientation occurs.

Temperature dependences of magnetization of $Mn_{3.4}Ag_{0.6}N$ and Mn_3AgN, under the dc magnetic field of 10 mT and 5 T, respectively, are plotted in Fig. 4a. The same dependences at low temperatures are shown in Fig. 4b. Under the field of 10 mT, the magnetic behaviour of Mn_3AgN is similar to that of $Mn_{3.4}Ag_{0.6}N$ above 20 K. That is, they display a cusp at 275 and 256 K, respectively. But below 20 K, the magnetization of $Mn_{3.4}Ag_{0.6}N$ becomes large again, while that of Mn_3AgN becomes continuously smaller. Under the field of 5 T, similar behaviours of both compounds can be distinctly observed throughout the whole temperature range, other than the rounder peaks (see the upper panel of Fig. 4a).

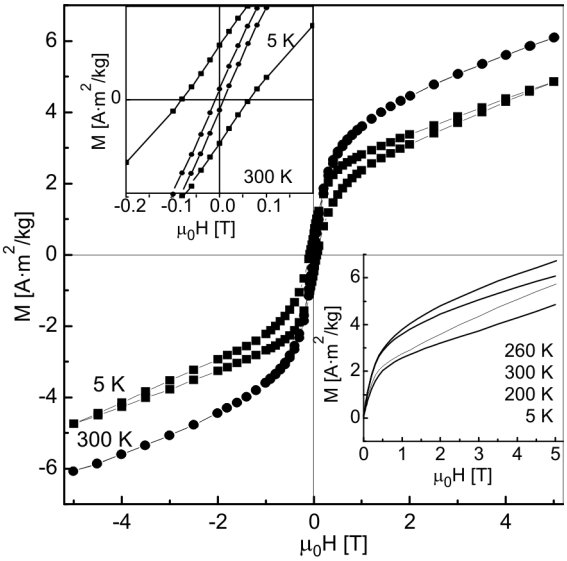

Fig. 5. Hysteresis loops of Mn_3AgN at 5 and 300 K. The top inset shows the hysteresis loops at 5 K and 300 K in a larger scale, while the bottom one isothermal magnetization curves at various temperatures

Fruchart et al. [9] reported that, for Mn_3AgN compounds, a combination of two triangular AFM structures, i.e. Γ^{4g} and Γ^{5g}, exists below 55 K, while an entirely triangular AFM Γ^{5g} structure exists between 55 and 290 K. This indicates that a magnetic change occurs at about 55 K. According to Gomonaj et al. [10] this magnetic transition should be from triangular AFM to FIM nc upon decreasing temperature. For $Mn_{3.4}Ag_{0.6}N$, below 20 K, the magnetization enhancement suggests the occurrence of the magnetic transition, essentially consistent with the findings in Refs. [9] and [10]. For Mn_3AgN under low field, the smaller magnetizations with decreasing temperatures seem to be associated with the enhancement of magneto-crystalline anisotropy which is evident as shown in the top inset of Fig. 5. Under a strong field, Mn_3AgN

displays the same behaviour as that of $Mn_{3.4}Ag_{0.6}N$ which reveals that both compounds should experience similar magnetic transitions. On the other hand, the peaks at 256 and 275 K, for the magnetizations of $Mn_{3.4}Ag_{0.6}N$ and Mn_3AgN, respectively, indicate that both the compounds exhibit different magnetisms below and above these temperatures.

The hysteresis loops of Mn_3AgN at 5 and 300 K are plotted in Fig. 5. Below 1 T, they both display ferrimagnetic-like behaviour, while AFM behaviour can be observed under a strong field, which is a common characteristic of Mn_3MN (M = Sn, Ag, Ni, et al.) [4, 10, 16]. The bottom inset represents the isothermal magnetizations of Mn_3AgN at various temperatures. As temperature increases, the magnetization becomes enhanced in the range from 5 to 260 K, and gets small again above 260 K, implying that the magnetic transition can occur at 260 K, corresponding to the observation of the isofield magnetizations. However, this magnetic transition seems to only relate to the comparative increase/decrease of the ferromagnetism component of Mn_3AgN.

Commonly, the triangular spin configuration per unit is composed of three spin vectors, with their respective angle of 120º. The triangle rotates opposite to the rotation of the field [18]. Moreover, the aforementioned triangular AFM is based on the symmetry of Γ_{4g} or Γ_{5g}, or their combined magnetic structures. When a strong magnetic field is exerted on this configuration, the three spins will be partially aligned along the direction of the field. Therefore, ferrimagnetic-like behaviour will gradually increase, based on the increasingly weakening magneto-crystalline anisotropy in function of increasing temperature. Finally, once the $M(T)$ curves achieve peak magnetization (i.e., those when a maximum vector sum is attained) under the 5T field, magnetization decreases with subsequent temperature increase. To some extent, this process is the magnetic transition from triangular AFM Γ^{5g} structure to ferrimagnetic-like one, but at a gradual pace. This argument can be used to explain the magnetic behaviour of $Mn_{3.4}Ag_{0.6}N$ and Mn_3AgN compounds above 200 K.

3.3. Transport properties

Temperature dependences of electrical resistivity of Mn_3AgN under the fields of 0 and 5 T, respectively, are shown in Fig. 6. Its inset shows the temperature dependence of magnetoresistance MR. It is noted that the electrical resistivity is rather large. Furthermore, a double minimum of resistivity occurs on the $\rho(T)$ curves. As is known, the compound experiences a magnetic transition from AFM to FIM n.c. at low temperatures. Based on the magnetic scattering mechanism, the electrical resistivity should become small, contrary to our observation. In fact, the spin-glass-like and ferrimagnetic phases of $Mn_{4-x}Ga_xN$ solid solution ($0.7 < x < 1$) [11] always coexist at low temperatures which arises from a complicated change of magnetic structures. We conjecture that the enhancement of electrical resistivity for Mn_3AgN at low temperatures is due to the presence of such disorder as spin glass or spin-glass-like phase.

Between 45 and 220 K (the temperature corresponding to the maximum electrical resistivity), the resistivity becomes enhanced with increasing temperature. In the same temperature range, the magnetization increases almost linearly, which is characteristic of triangular AFM. The increase of the resistivity reveals the enhancement of AFM. From 220 to about 350 K, the magnetic measurement reveals the gradual magnetic transition from triangular AFM Γ^{5g} structure to a ferrimagnetic-like one. Correspondingly, the resistivity exhibits the contrary process.

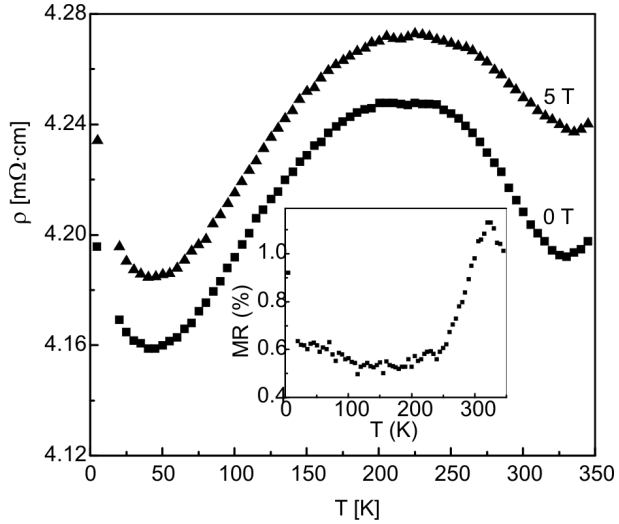

Fig. 6. Temperature dependences of electrical resistivity of Mn_3AgN at various fields. The inset represents temperature dependence of MR value, i.e. $(\rho(H) - \rho(0))/\rho(H)$, where $\rho(H)$ and $\rho(0)$ correspond to the electrical resistivities measured in dc magnetic fields of 5 T and 0 T, respectively

In terms of the above measured results, MR value can be determined, which is plotted in function of temperature in the inset of Fig. 6. The zero-field electrical resistivity curve is almost the same as that corresponding to a 5 T dc field. Furthermore, the latter is above the former in the whole temperature range, which means a positive MR value, with the maximum of 1.13%. Chi et al. [3] reported a positive MR value of $CuNMn_3$ in the whole temperature range, with the maximum of 4% at 150 K under the field of 5 T. According to Kim et al. [2], for $ZnNMn_3$ compound, the structure-induced magnetic transition can result in the increase/decrease of the electrical resistivity. That is, micro-cracks, generated from the irreversible radical lattice expansion can lead to the enhancement of resistivity and a positive MR value. Sun et al. [19] reported an anomalous, positive-valued MR in $Fe_{0.75}Mn_{1.35}As$. By combining the lattice expansion, confirmed by XRD measurement, with the magnetic measurements, they unambiguously revealed that micro-cracks resulting of radical lattice expansion are the dominant factor leading to positive MR. Our Mn_3AgN compound was prepared by milling and subsequently annealed at 823 K for 30 min. The presence of a broad XRD peak reveals that the homogenization is rather insufficient for removing the de-

fects such as dislocations, stacking faults, grain boundaries, etc., arising from the high-energy milling process. Therefore, it seems that the presence of a magnetic field is not the only factor leading to the positive MR value. The so-called magnetoresistance can also arise from other non-field contributions, such as micro-cracks.

4. Conclusions

By means of milling and subsequent annealing the mixture of $Mn_2N_{0.86}$, Mn, and Ag powders, $Mn_{4-x}Ag_xN$ (x = 0.0, 0.3, 0.6, 1.0) compounds were successfully prepared. All samples exhibit single-phase compounds. Mn_4N and $Mn_{3.7}Ag_{0.3}N$ display ferrimagnetism. Partial Ag replacement of Mn can promote the saturation magnetization. For $Mn_{3.4}Ag_{0.6}N$ and Mn_3AgN compounds, the magnetic transition below 15 K is from AFM to FIM n.c. with lowering temperature. The magnetic transitions at 256 and 275 K, respectively, can be ascribed to the gradual transition from triangular AFM Γ^{5g} structure to ferrimagnetic-like one. Two minima occur on the curves of temperature dependences of electrical resistivity which can be clearly interpreted by the magnetic scattering mechanism. Positive magnetoresistance can be observed in the whole temperature range, with the maximum of 1.13%.

Acknowledgements

This work has been supported by the National Natural Science Foundation of China under Grant No. 50331030, and by the Liaoning Province Science Foundation of China under Grant No. 20070556.

References

[1] BOUCHAUD J.P., Ann. Chim., 3 (1968), 81.
[2] KIM W.S., CHI E.O., HUR N.H., LEE K.W., CHOI Y.N., Phys. Rev. B, 68 (2003), 172402.
[3] CHI E.O., KIM W.S., HUR N.H., Solid State Commun., 120 (2001), 307.
[4] FENG W.J., LI D., REN W.J., LI Y.B., LI W.F., LI J., ZHANG Y.Q., ZHANG Z.D., J. Alloy. Compd., 437 (2007), 27.
[5] MAH A.D., J. Am. Chem. Soc., 80 (1958), 2954.
[6] TAKEI W.J., SHIRANE G., FRAZER B.C., Phys. Rev., 119(1) (1960), 122.
[7] TAKEI W.J., HEIKES R.R., SHIRANE G., Phys. Rev., 125(6) (1962), 1893.
[8] VEMPAIRE D., FRUCHART D., GOUTTEBARRON R., HLIL E.K., MIRAGLIA S., ORTEGA L., PELLETIER J., Physica A, 358 (2005), 136.
[9] FRUCHART D., BERTAUT E.F., J. Phys. Soc. Jpn., 44(3) (1978), 781.
[10] GOMONAJ E.V., L'VOV V.A., Phase Trans., 40 (1992), 225.
[11] NAVARRO R., ROJO J.A., GARCÍA J.J., GONZÁLEZ D., BARTOLOMÉ J., L'HERITIER PH., J. Magn. Magn. Mater., 59 (1986), 221.
[12] TAKENAKA K., TAKAGI H., Appl. Phys. Lett., 87 (2005), 261902.
[13] TAKENAKA K., TAKAGI H., Mater. Trans., 47 (3) (2006), 471.
[14] FENG W.J., SUN N.K., GAO M., ZHANG Q., DENG Y.F., ZHANG Z.D., Physical B, in press.
[15] MEKATA M., J. Phys. Soc. Jpn., 17 (1962), 796.

[16] GOMONAJ E.V., Phase Trans., 18 (1989), 93.
[17] GOMONAJ E.V., L' VOV V.A., Phase Trans., 38 (1992), 15.
[18] TOMIYOSHI S., YAMAGUCHI Y., J. Phys. Soc. Jpn. 51,(1982), 2478.
[19] SUN N.K., LI Y.B., LI D., ZHANG Q., FENG W.J., ZHANG Z.D., Phys. Rev. B 74 (2006), 172402.

Received 15 October 2007
Revised 19 December 2008